Synthesis, Characterization and Study of Electrical Properties of Polyaniline-NiO Nanocomposites

Rajashekhar B[1]

Assistant Professor,

Department of chemistry,

KLE Dr MS Sheshgiri College of Engineering & Technology,

Belgaum-590008, Karnataka, India.

Vishnuvardhan T K[2]

Assistant Professor & Head,

Department of Chemistry,

Acharya Institute of Technology, Bangalore-560107, Karnataka, India.

Shashidhar N[3]

Associatete Professor

Department of Chemistry,

SDM College of Engineering & Technology, Dharwad-580002, Karnataka, India.

Satishkumar K B[4]

Assistant Professor,

Department of Chemistry,

Acharya Institute of Technology, Bangalore-560107, Karnataka, India.

Basavaraja C[5]

Professor,

Department of Chemistry,

Inje University, Kyungnam-621749, South Korea.

Chandrashekhar M[6]

Assistant Professor,

Department of Physics,

Acharya Institute of Technology, Bangalore-560107, Karnataka, India.

Abstract: NiO Nanoparticles (NNP) were synthesized by a self propagating high temperature synthesis from nickel nitrate. Synthesized NiO are used to prepare Polyaniline (PANI)-NiO nanocomposites by in situ chemical oxidative polymerization at 0-5^0C. Different weight percentages of NiO (10%, 20%, 30% and 40%) were added during the polymerization. The nanocomposites were characterized by X-Ray diffraction (XRD) and Fourier Transform Infrared (FTIR) and UV Techniques. Crystallite strain is calculated from Williamson-Hall(WH) method using XRD data. Surface morphology was studied using Scanning Electron Microscopy (SEM) and EDAX. Frequency dependent AC conductivity and dielectric properties of PANI-NNP composites were analyzed in the frequency range 50–10^6 Hz at room temperature. These nanocomposites have microwave, sensor and battery applications.

Key words: *Nanoparticles, self propagating high temperature synthesis, peak width analysis, conductivity and dielectric properties.*

1. Introduction:

NiO is a magnetic and highly conducting material [Kim YS et.al., 2003]. Preparation of NiO or other modified NiO nanoparticles find application in the magnetic and recording materials, photoelectric, sensor etc., due to their special structural properties [Shi JJ et.al., 2004, Li X, et.al, 2013, Singh J, 2011]. The development of intrinsically conducting polymers (CPs)[Alan JH, 2001] has received much attention because of their potential applications in electrochromic devices[Sapp S A et.al., 1996], sensors[Li J et.al., 2013], super capacitors, rechargeable batteries[Giri S, et.al., 2013] microwave applications[Basavaraja C et.al., 2011] and so on. Research in the field of such polymer aims mainly at some suitable modifications of existing polymers so that their applicability can be improved. Addition of metal oxide[Hanemann T, 2010] to PANI gives excellent mechanical strength, conductivity, dielectric behavior[Wang S, 2011] to PANI[Lonergan MC, 1997, Vishnuvardhan TK et.al., 2006]. Some of these modifications include preparing hybrid materials involving organic materials and inorganic oxides or salts of different metals[Pande S et.al., 2012, Nandapure BI et.al., 2013, Mahesh B et.al., 2010, Song JH et.al., 2013]. These are known as polymer composites[Mimani T et.al., 2001, Basavaraja C et.al.]. Among the conducting polymers, polyaniline(PANI) is considered to be the most promising material because of its unique properties such as controllable and relatively high conductivity, high electrochemical activity[Sultana S et.al., 2012], ease of synthesis[Kebichea H et.al., 2012], lower cost[Ansari R et.al., 2006], good environmental stability[Ramamurthy PC et.al, 2004]. In recent years NiO nanoparticles are gaining much importance due to their magnetic properties [Kodama RH et.al., 1997, Kodama RH, 1999,]. Also Non-stoichiometric nickel oxide exhibits good P-type semiconducting properties owing to its defect structure [Palombari R, 2003]. It's a NaCl type antiferromagnetic oxide semiconductor[Marselin. M. A., 2014-2015]. There are several methods of synthesis of NiO nanoparticles such as sol-gel[Ying W et.al., 2007, Schiffrin D.J., 2001], solvothermal [Beach E.R et.al., 2009], polymer-matrix assisted synthesis [Deki S. et.al., 2003] etc .
SHS is an efficient, low-cost and self purifying method which evolves soft and fine nanoparticles with high surface area and different surface properties [Shakir M et.al., 2009, Aruna ST et.al., 2008]. In this paper, NiO nanoparticles (NNP) are prepared by self-propagating high- temperature synthesis (SHS). Such synthesized nanoparticles have a distinct surface property impact on dielectric and conductivity. Synthesis of PANI is done at 0-5^0 C in Emeraldine salt form by chemical oxidative polymerization method with controlled pH 3 by using Ammonium peroxydisulphate. NNP is blend with PANI by chemical oxidation method and varied amount of NNP are put to get varied composites of NiO-PANI composites. The prepared nanocomposites were characterized by Fourier Transform Infrared (FTIR) and X-Ray Diffraction (XRD) Techniques. WH method is used for justifying crystallite size determined by using Scherrer Equation and crystallite strain which is

obtained from the peak width analysis. Surface morphology was studied using Scanning Electron Microscopy (SEM).

Frequency dependent AC conductivity, dielectric constant and dielectric loss are studied in the range of 50 Hz to 1 MHz at room temperature. These properties are important to decide sensor activity, battery applications and microwave properties.

2. Experimental:

Materials: All chemicals used are AR grade. Precursor $Ni(NO_3)_2.6H_2O$ from Hi-media. Urea as a fuel, Ammonium persulfate(APS) as a oxidant, Monomer Aniline, ethanol(anhydrous), HCl, were purchased from Fischer Scientific. Aniline used after distillation.

2.1 Method :

Synthesis of NiO Nanoparticles: Aqueous solutions of precursor $Ni(NO_3)_2.6H_2O$ and fuel Urea are added in the stoichiometric ratio of 1:1.6 taken in 100ml capacity glass crucible. Heated to 350-500 ^{0}C in a muffle furnace for 1 hour and cooled to room temperature. Obtained NiO nanoparticles is collected, calcined for 2 hrs at 600 ^{0}C.

Synthesis of PANI-NiO nanocomposites: Weighed amount of NiO is dispersed in de-ionised water and 0.06 mole of monomer is added slowly. 100 ml of 0.2 mole Ammonium persulfate as oxidizer is added drop wise with stirring and the reaction is performed for 2 hours. Temperature is maintained at 0-5 ^{0}C during the polymerization. The precipitated polymer composite is filtered, washed with de-ionised water several times and then with 5% ethanol. Different weight percentages of NiO is added during the polymerization to get PANI-5% NiO(PN-5), PANI-10% NiO(PN-10), PANI-20% NiO(PN-20), PANI- 30% NiO(PN-30) and PANI-40% NiO(PN-40).
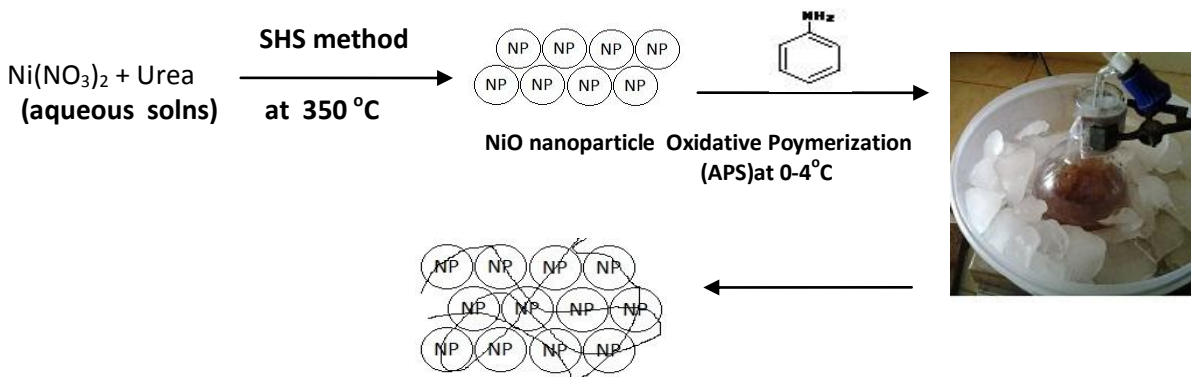

Encapsulation of NiO nanoparticles by polyaniline

Figure 1: Schematic Diagram showing the synthesis of PN nanocomposites

2.2 Instrumentation: The synthesized NiO nanoparticles were characterized by the following. Fourier transformed infrared (FT-IR) spectroscopy by using Bruker optic GMBH tensor 27 spectrometer, KBr used for the palate for the absorbance in the range of 4000-600 cm^{-1}. X–ray powder diffraction (XRD) by using a Bruker D2 Phraser diffractometer with Cu-Kα radiation (λ=1.54 Å) 4° to 80°. Scanning electron microscopy (SEM) technology accompanied by Energy dispersive X-ray (EDX) analysis was performed on GEMINI ULTRA 55. AC conductivity for the synthesized nanocomposites was measured using Keithley automatic electrometer.

3. Results and Discussions:

IR : Fig.2 (a- e): shows the FTIR spectra of pure PANI, PN-5, PN-10, PN-20, PN-30, PN-40 composites and pure NiO nanoparticles, which showed significant absorption peaks at 1298, 1497, 1243, 1346, 1041 and 818 cm^{-1} correspond to polymerized aniline. The band at 818 cm^{-1} attributed to out of plane bending vibration of C-H bond of p-substituted benzene ring. The bands corresponding to stretching vibrations of benzenoid and quinoid moieties in the polyaniline backbone appear at 1497 and 1573 cm^{-1}, respectively. The peak appeared at 1145 cm^{-1} corresponds to protonated state of polyaniline. The absorption band at 1243 cm^{-1} is associated with polaronic structure of PANI. The bands at 1147 cm^{-1} correspond to polyaniline in the composites. The bands corresponding to vibration mode of quinoid ring and stretching mode of C-N bond appear at 1147 and 1346 cm^{-1}, respectively. Similar peaks observed in composites indicate the formation composites metal oxygen and polymer binded by Van der Waals interaction. Broad absorption band in the region of 631–772cm^{-1} is assigned to Ni–O stretching vibration mode; the broadness of the absorption band indicates that the NiO powders are nanocrystals. All these IR data are in good agreement with reported one.
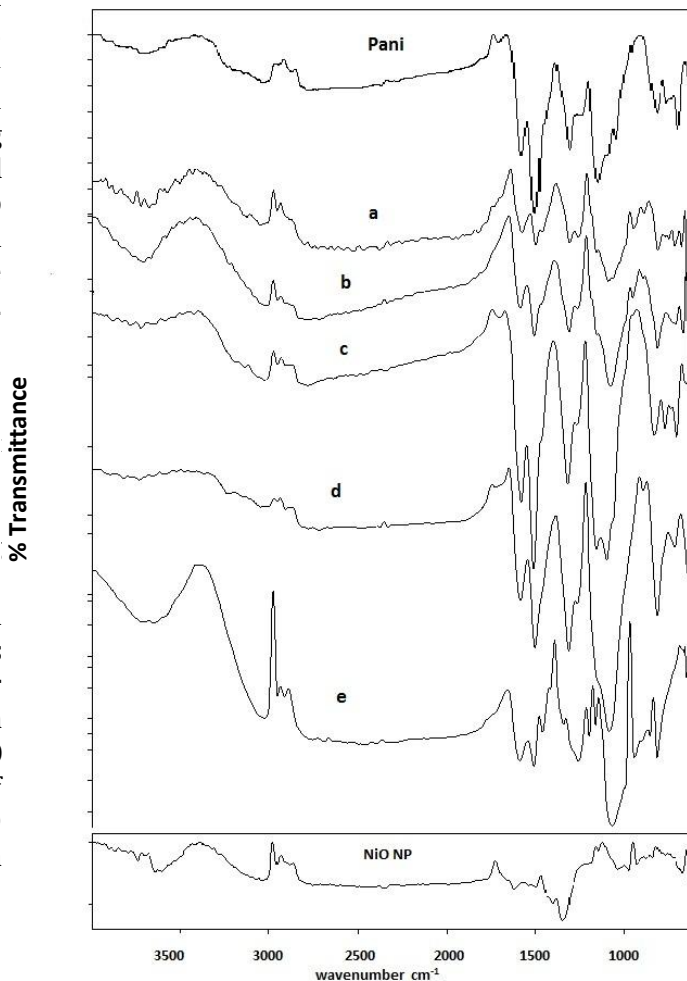

Figure 2: FT-IR spectra of Pure PANI and a)PN-5 b) PN-10 c) PN-20 d) PN-30 and e) PN-40 a) NiO NP.

XRD :

Synthesized NiO nanoparticles were examined by using powder X-ray diffraction (XRD) as shown in Fig.3. The XRD peak for polyaniline is broad due to amorphous nature of the polymer. Low and broad diffraction peaks indicate small size effect and incomplete inner structure of the particle. The peaks appearing at 2θ= 37.2, 43.20, 62.8, 75.2, and 79.3 can be readily indexed as (111), (200), (220), (311), and (222) crystal planes of the bulk NiO, respectively. In addition to these peaks in the composites, there is a broad peak appeared for polymerized aniline. As the percentage of metal oxide increases in composites, peaks due to nickel oxide is pronounced along with the pure PANI peak. All these diffraction peaks can be perfectly indexed to the face-centered cubic (FCC) crystalline structure of NiO, not only in peak position, but also in their relative intensity of the characteristic peaks, which is in accordance with that of the standard spectrum (JCPDS, No. 04-0835). The NiO lattice constant calculated from the XRD data is in agreement with the reported data [Zak AK et.al., 2011]. Further when compared to pure PANI and pure metal oxide with the composites, both the peaks exist in the composites.
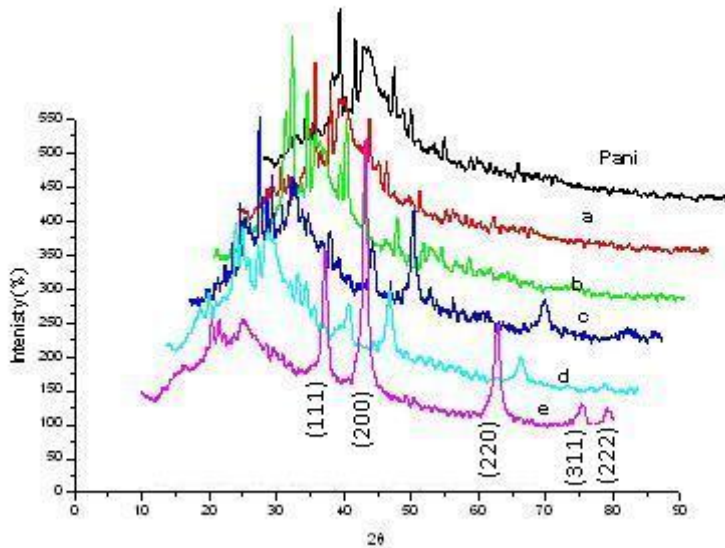
Figure 3: XRD pattern of Pure PANI a) PN-5 b) PN-10 c) PN20 d) PN-30 and e) PN-40

The particle size of all the composites is calculated and tabulated in Table 1 from Scherrer Equation $D = \frac{k\lambda}{\beta cos\theta}$ .Where, D is the particle size in nm, λ is the wavelength of the radiation(=1.54 Å), β is the Full Width at Half Maximum intensity, θ is the peak position and k is a constant equal to 0.9. Williamson-Hall method (WH method) was used to calculate particle size and strain induced broadening. In this method graph was plotted with βcosθ Vs 4sinθ and slope was determined, which is in good agreement with that calculated from Scherrer Equation. The Table 1 provides the particle size of nanocomposites as calculated from both the methods. Further, size-strain plot model for each of the synthesized PN composites from WH plot gives the strain induced broadening value in the order of 0.123 to 0.344. It is observed that the strain induced in composites during polymerization varies from one composite to another composite depending on their size. In this study it is seen that as the crystallite size of particle decreases, strain induced in the composites increases.

Table 1: Particle size as calculated from Scherrer Equation and WH plots using XRD pattern for

PN-composites

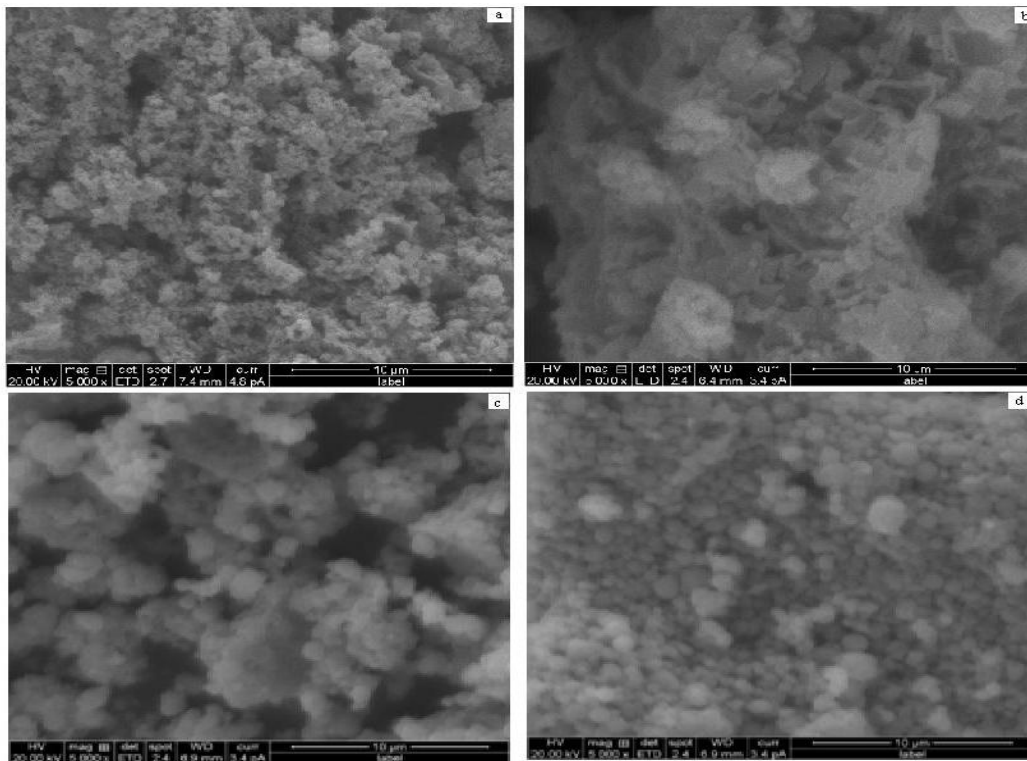| Sl.No.	Composite	Particle size from-Scherrer Equation	Particle size from Williamson-Hall method	Strain induced broadening
1	PN-10	43.58 nm	39.8 nm	0.123
2	PN-20	29.87 nm	31.4 nm	0.344
3	PN-30	25.6 nm	24.1 nm	0.267
4	PN-40	24.9 nm	22.7 nm	0.335

SEM :

Figure 4: SEM images for PANI NiO composites a) NiO NP b)PN- 5 and c) PN-20 and d) PN-40.

Fig. 4 shows sem images of 5K Magnification for PureNiO, PN-5, PN-20 and PN-40 nano composites. Fig. 4a shows small spherical shaped Pure NiO. Fig. 4b of PN-5 shows the encapsulation of NiO nano particles by polyaniline with flower like structure. Fig. 4c and 4d for PN-20 and PN-40 respectively depicts spherical shaped structures with cluster formation.
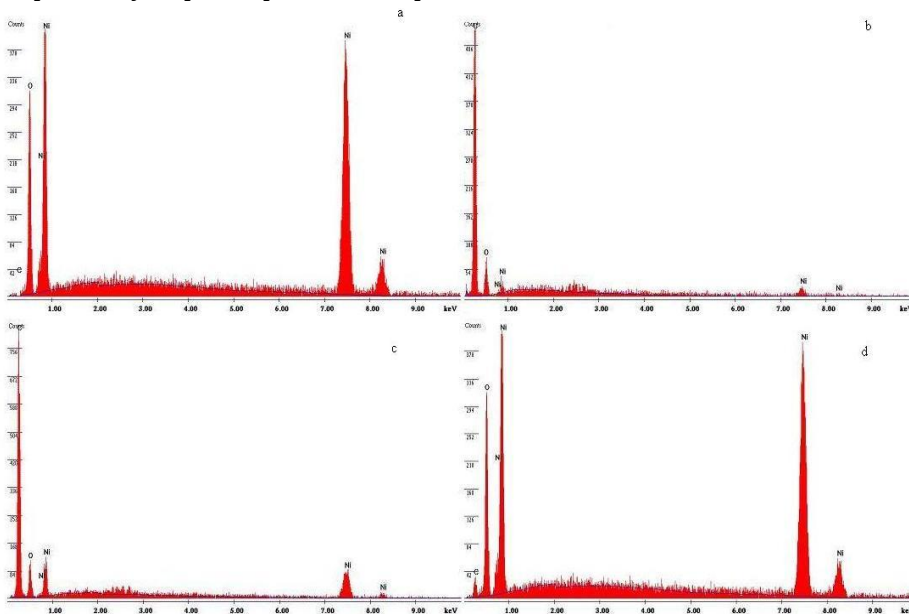

Figure 5: EDAX spectra for PANI NiO composites a) NiO NP b)PN- 5 c) PN-20 and d) PN-40.

Fig. 5a shows the edax of the pure NiO nano particles, in which the peaks for Ni and oxygen indicates the purity of the NiO. Fig. 5b, 5c and 5d shows the PANI NiO peaks for PN-5 and PN-20 and PN-40 respectively. Presence of NiO and aniline can be confirmed from the count.

AC conductivity: Fig.6 shows the frequency dependent AC conductivity of PANI and PN composites. Conductivity of PANI and PANI composites remains same upto the frequency of 10^5 Hz then onwards there is the increase in the conductivity at higher frequency. Maximum conductivity showed for PN-10 samples may be due to the chain length that can be confirmed from IR and XRD graph. Increased conductivity may be due to increased charge polarization. Fig.7 shows the how PN-10 is distinctly high conductivity showed compared to other composites with 1Mega Hz frequency level and quantitative change in the conductivity with respect to different frequency level also depicted.
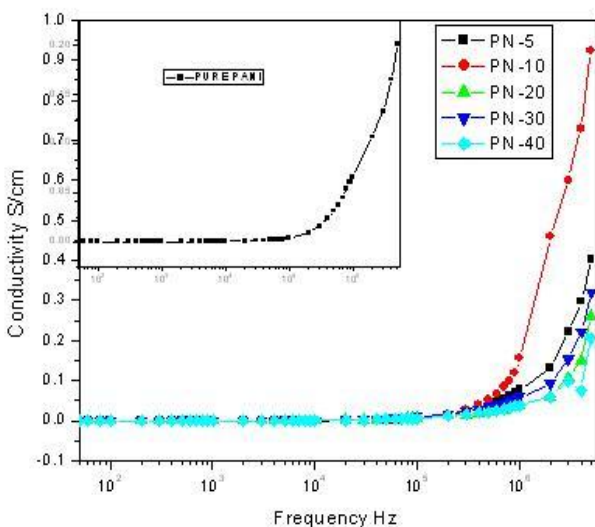

Figure 6: Frequency dependent AC conductivity of PANI(inset figure) and PANI composites a)PN-5 b) PN-10 c) PN-20 d)PN-30 e)PN-40
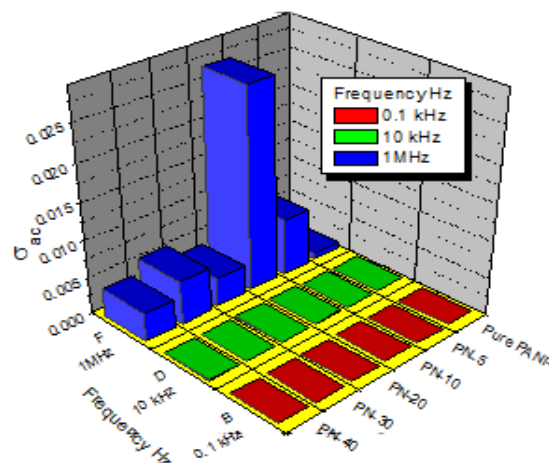
Figure 7 : Variation of AC conductivities of PN-composites at three different frequencies.

Dielectric constant:

Dielectric property of the PN composites are shown in the Fig.8. At lower frequency PN-10 sample shows higher dielectric constant. As the frequency increases all the composites show saturated dielectric constant. At saturated level PN-30 exhibits highest dielectric constant. Inset of the Fig. 8 shows dielectric constant for Pure PANI. Composites show higher dielectric constant than pure PANI. Fig. 9 shows bar chart for the PN samples at three different frequencies.
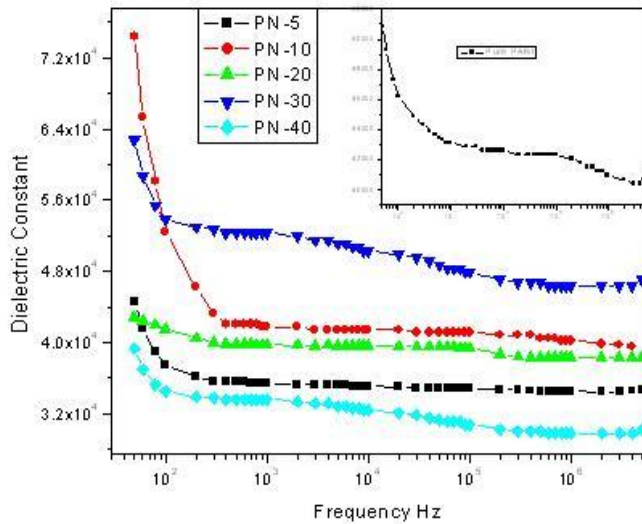
**Figure 8: Frequency dependent dielectric constant
of PANI(inset figure) and PANI composites
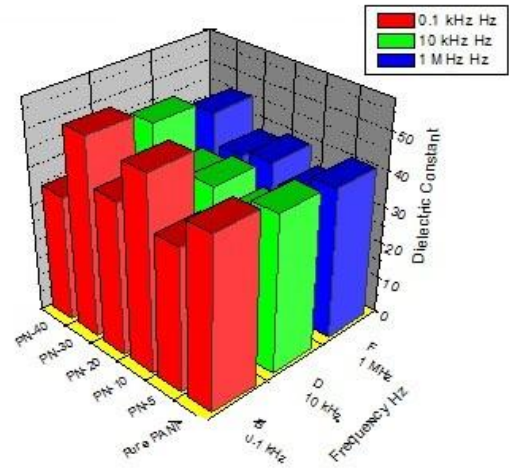a)PN-5 b) PN-10 c) PN-20 d)PN-30 e)PN-40**

**Figure 9: Variation of dielectric constant of
PN-composites at three different
frequencies.**

Dielectric Loss: Dielectric loss of the PN composites are shown in the fig.10. At lower frequency PN-5 sample shows higher dielectric loss as the frequency increases all the samples shows saturated dielectric loss, at saturated level almost all samples show saturated dielectric loss. Inset of the fig. 10 shows dielectric loss for Pure PANI. Composites show higher dielectric loss than pure PANI. Fig. 11 shows bar chart for dielectric loss the PN composites at three different frequencies.
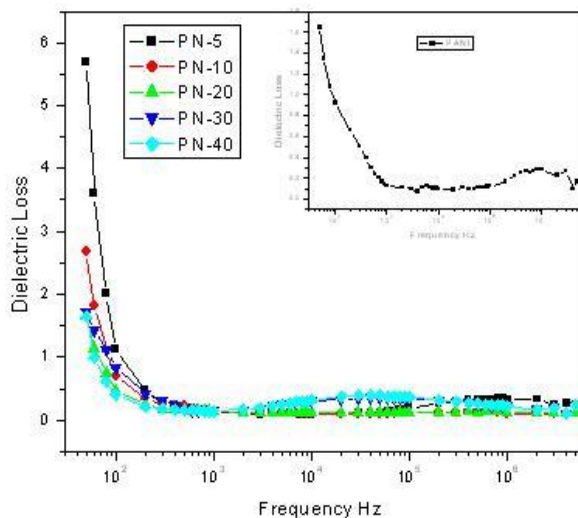

**Figure 10: Frequency dependent Dielectric Loss
of PANI(inset figure) and PANI composites
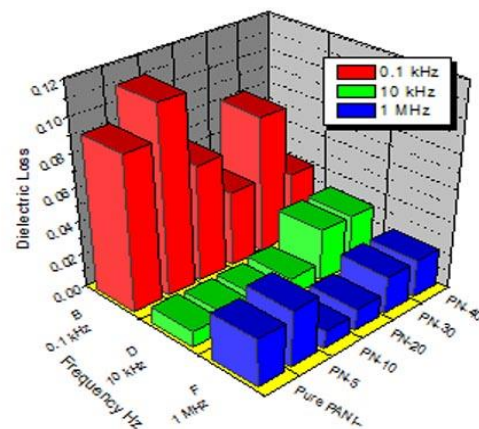a)PN-5 b) PN-10 c) PN-20 d)PN-30 e)PN-40**

**Figure11: Variation of Dielectric Loss of
PN-composites at three different
frequencies.**

4. Conclusions: NiO nanoparticles are synthesized by SHS method. These synthesized NNP are used to blend with PANI to get PANI -NiO (PN) composites and the resulting composites are characterized. FTIR shows weak Van der Waals forces of attraction between metal oxide and polymerised aniline. The particle size of composites are calculated from Scherrer's equation using intense peaks from XRD . The average particles size ranges from 24.9 nm to 43.6 nm and confirms the presence of NiO and polyaniline and verified by WH method. WH method reveals that strain is induced in composites during polymerization. This may be the reason for variation in conductivity of the nanocomposites. SEM images show the encapsulation of the metal oxide by PANI and cluster formation. EDAX spectra shows the purity of the composites. PN-10 composite shows high conductivity and dielectric constant which may be due particle size. Conductivity and dielectric behaviour of the above synthesized nanocomposites suites for the battery applications.

References:

1. Kim Y.S., Kim Y.H., 2003, Application of ferro-cobalt magnetic fluid for oil sealing, *J. Magn.Magn. Mater.,* 267, 105.
2. Shi, J.J., Zhu. Y.F., Zhang. X.R., Willy. R.G.B., Ana. R.G.C., 2004, *Trac-Trends Anal. Chem.*23, 351.
3. Li. X., Zhang. L., Wei. X., Li. J., 2013, A Sensitive and Renewable Chlortoluron Molecularly Imprinted Polymer Sensor Based on the Gate-Controlled Catalytic Electrooxidation of H_2O_2 on Magnetic Nano-NiO, *Electronanlyis*, 25(5) 1286.
4. Singh. J., Kaliata. P., Singh. M.K., Malhotra. B.D., 2011, Nanostructured nickel oxide-chitosan film for application to cholesterol sensor, *Appl. Phys. Lett.* 98, 123702.
5. Alan. J.H., 2001, Semiconducting and metallic polymers: the fourth generation of polymeric materials, *The Jl. Of Phys. Chem.B.,*105, 36, 8475.
6. Sapp. S. A., Sotzing. G. A., Reddinger. J. L., Reynolds. J.R., 1996, Rapid switching solid state electromic devices based on complementary conducting polymer films, *Adv. Mat.,*8 (10) 808.
7. Li.J., Liu. S., Yu. J., Lian.W., Cui. M., Xu.W., Huang. J., 2013, Electrochemical immunosensor based on graphene–polyaniline composites and carboxylated graphene oxide for estradiol detection, *Sens. Actuators B: Chemical*, 188, pp 99-105.
8. Giri. S., Ghosh. D., Das. C.K., 2013, In situ synthesis of cobalt doped polyaniline modified graphene composites for high performance supercapacitor electrode materials, *J. Electroanal. Chem.*, 697, pp 32-45.
9. Basavaraja.C., Jo. E.A., Kim.B.S., Kim. D.G., Huh.D.S., 2011, Microwave absorption of poly-*N*-vinylcarbazole-polyaniline composites *Polym. Engg. Sci.*, pp 55-61.
10. Hanemann.T., Szabo. D.V., 2010, Polymer-Nanoparticle Composites: From Synthesis to Modern Applications, *Materials*, *3*, pp 3468-3517.
11. Wang.S., Gao. Q., Zhang. Y., Gao. J., Sun. X., Tang. Y., 2011, Controllable Synthesis of Organic-Inorganic Hybrid MoO*x*/Polyaniline Nanowires and Nanotubes, *Chem.Eur.J.*,17, pp 1465-1472.
12. Lonergan. M.C., 1997, A Tunable Semiconductor Diode Based on an Inorganic Semiconductor -Conjugated Polymer Interface, *Science*, 278, pp 2103-2106.
13. Vishnuvardhan. T.K., Kulkarni. V.R., Basavaraja. C., Raghavendra. S.C., 2006, Synthesis, characterization and a.c. conductivity of polypyrrole/Y2O3 composites, *Bull.Mater. Sci.*, 29,1,77-83.
14. Pande.S., Mahesh S.H., Bedre. D., Bhat. R., Deshpande. R., Venkataraman. A., 2012, Synthesis, Characterization and Studies of PANI-MMT Nanocomposisites, *Nanosci. Nanotech.,* 2(4): 90-98. DOI:10.5923/j.nn.20120204.01.

15. Nandapure. B. I., Kondawar. S. B., Salunkhe. M.Y., Nandapure. A.I.,2013, Magnetic And Transport Properties Of Conducting polyaniline/nickel Oxide Nanocomposites *Adv. Mat. Lett.*, 4(2), pp 134-140. DOI: 10.5185/amlett.2012.5348.

16. Mahesh.B., Basavaraja.S, Raghunandan.D., Balaji.S., Arunkumar.L., Govindraj.B., Venkataraman. A., 2010, *J. Metallurgy Mater. Sci.,*52,(2), pp149-154. ISSN : 0974-1267.

17. Song. J.H., Park. M.Y., Lim. H.T., 2013, Single-step preparation of nano-homogeneous NiO/YSZ composite anode for solid oxide fuel cells. *Nano-Micro Lett.*, 5(2), pp 111-116.

18. Mimani.T., Patil. K.C., 2001, Solution Combustion Synthesis Of Nanoscale Oxides And Their Composites *Mater.Phys.Mech,* 4, pp 134-137.

19. Basavaraja. C., Veeranagouda. Y., Lee. K., Pierson. R., Huh. D. S., Surface characterization and electrical behavior of polyaniline-polymannuronate nanocomposites, *J. Polym. Sci.:Part B Polym. Phy.,* DOI 10.1002/polb.

20. Sultana. S., Rafiuddin, Khan. M.Z., Umar. K., 2012, Synthesis and characterization of copper ferrite nanoparticles doped polyaniline, *J. Alloys Compd,*535, pp 44-49.

21. Kebichea. H., Debarnota. D., Merzoukib. A., Poncin-Epaillarda. F., Haddaoui. N.,2012, Relationship between ammonia sensing properties of polyaniline nanostructures and their deposition and synthesis methods, *Anal. Chim.Acta.,*737, pp 64-71.

22. Ansari. R., Keivani. M.B., 2006, Polyaniline-Conducting Electroactive Polymers: Thermal and Environmental Stability Studies, *E-J. Chem.* 3, (13), pp 202-217.

23. Ramamurthy. P.C., Malshe. A.M., Harrell. W.R., Gregory. R.V., McGuire. K., Rao. A.M., 2004, Polyaniline/single-walled carbon nanotube composite electronic devices, *Solid- State Electron.* 48, pp 2019-2024.

24. Kodama. R.H., Makhlouf. S.A., Berkowitz.A, 1997, Finite size effects in antiferromagnetic NiO nanoparticles, *Phys. Rev. Lett.,* 79, 1393.

25. Kodama. R.H., 1999, Magnetic nanoparticles, *J. Magn. Magn. Mater.* 200, 359.

26. Palombari.R., 2003, Influence of surface acceptor–donor couples on conductivity and other electrochemical properties of nonstoichiometric NiO at 200 °C, *J. Electroanal.Chem.,*546,23.

27. Marselin. M. A., Jaya. N.V., 2014-2015, Synthesis and characterization of Pure and Cobalt-doped NiO Nanoparticles, *Int.J. ChemTech. Res*.,7(6),2654-2659.

28. Ying W., Yiming H., Tinghua W., Weizheng W., Huilin W., Effect of synthesis method on the physical and catalytic property of nanosized NiO, 2007, *J. Mater. Lett.,*62, 2679-2682.

29. Schiffrin D.J., 2001, Capped nanoparticles as potential electronic components with nanoscale dimensions, *MRS. Bull.,* 26, pp 1015-1019.

30. Beach E.R., Shaue K.R., Brown S.E., Rozesveld S.J. and Morris P.A, 2009, Solvothermal synthesis of

    crystalline nickel oxide nanoparticles, Mater. Chem. Phys. 115, 373-379.

31. Deki S., Yanagimito H., Hiraoka S., 2003, NH₂-terminated poly(ethylene oxide) containing nanosized NiO particles: Synthesis, Characterisation and structural considerations, *Chem.Mater.*,15, pp 4916-4922.

32. Shakir. M., Singh. B.K., Gaur. R.K., Kumar.B., Bhagavannarayana.G., Wahab. M.A., 2009, *Chalcogenide Letters*, 6,12,655-660.

33. Aruna. S.T., Mukasyan. A.S., 2008, Combustion synthesis and nanomaterials,*Curr. Opin. Solid State Mater. Sci.*,12, pp 44-50.

34. Zak. A.K., Majid A.W.H., Abrishami. M.E., Yousefi.R., 2011, X-ray analysis of ZnO nanoparticles by Williamson-Hall and size-strain plot Methods, *Solid State Sci.,*13, pp 251-256.